
DATA-DRIVEN EMOTIONAL BODY LANGUAGE GENERATION FOR SOCIAL ROBOTICS

Mina Marmpena
University of Plymouth
Plymouth, UK
mina.marmpena@itml.gr

Fernando Garcia
ANYbotics AG
Zurich, Switzerland
fgarcia@anybotics.ch

Angelica Lim
Simon Fraser University
British Columbia, Canada
angelica@sfu.ca

Nikolas Hemion
dSPACE GmbH
Paderborn, Germany
nhemion@dspace.de

Thomas Wennekers
University of Plymouth
Plymouth, UK
thomas.wennekers@plymouth.ac.uk

May 3, 2022

ABSTRACT

In social robotics, endowing humanoid robots with the ability to generate bodily expressions of affect can improve human-robot interaction and collaboration, since humans attribute, and perhaps subconsciously anticipate, such traces to perceive an agent as engaging, trustworthy, and socially present. Robotic emotional body language needs to be believable, nuanced and relevant to the context. We implemented a deep learning data-driven framework that learns from a few hand-designed robotic bodily expressions and can generate numerous new ones of similar believability and lifelikeness. The framework uses the Conditional Variational Autoencoder model and a sampling approach based on the geometric properties of the model’s latent space to condition the generative process on targeted levels of valence and arousal. The evaluation study found that the anthropomorphism and animacy of the generated expressions are not perceived differently from the hand-designed ones, and the emotional conditioning was adequately differentiable between most levels except the pairs of neutral-positive valence and low-medium arousal. Furthermore, an exploratory analysis of the results reveals a possible impact of the conditioning on the perceived dominance of the robot, as well as on the participants’ attention.

1 Introduction

In the near future more robots are expected to be deployed in social environments such as schools, care homes and shops. Their ability to interact socially with humans is becoming increasingly important [1] and as a consequence the field of social robotics is receiving increasing attention. Bartneck and Forlizzi [2] maintain that a social robot must adhere to “the behavioural norms expected by the people with whom the robot is intended to interact”, while Breazeal et al. [3] point out that social robots are expected to communicate with humans in an interpersonal manner, to engage them as partners, to collaborate or coordinate with them in order to accomplish positive outcomes. Among the characteristics of socially interactive robots identified by Fong et al. [4], we distinguish the ability to express and/or perceive emotions, establish/maintain social relationships, and exhibit personality and character. With our current work, we aim to facilitate these aspects of a social robot by endowing humanoid robots with the capability to display believable, diverse and appropriate emotional body language (EBL).

Body language is a subset of a broader group of nonverbal signals involved in human communication. Other such signals include facial expression or vocalizations. Facial expression is by far the most widely studied nonverbal signal of affect, with affective bodily expression lagging behind [5], although it constitutes a powerful communication channel among humans [6, 7, 8]. From a developmental point of view, body configurations are perceived from a

very early age [9], and they comprise the most primitive behavioural channel for humans to express emotion [10]. Compared to facial expression, EBL can reveal more about the actual affective state [11, 12, 10, 13], even when it is contradicted by facial expression and verbal communication [11]. Gestures and body postures evoke more trust [14], and they are less susceptible to social editing compared to facial expression [15]. Changes in a communicator’s body orientation, posture configuration, proxemics, etc. can influence the overall likeability, interest, and openness between individuals [11, 12, 16, 13]. Bodily expression of emotion has also been found more effective than facial expression in discriminating between intense positive and negative emotions [17] and in communicating emotion from a distance [18, 19].

These insights on the effects of human EBL, taken together with the human tendency to attribute anthropomorphic traits to non-human agents [20, 21, 22], support the hypothesis that the integration of robotic EBL in human-robot interaction (HRI) can enhance the user experience and make it more appealing and engaging [23]. Evidence from studies in HRI show that bodily expressions of affect can draw human’s attention [24], they are essential in naturalistic social interaction for robots that lack expressive faces (appearance-constrained) [25], and can make the interaction more enjoyable [26, 27].

Believable robotic EBL needs to be lifelike, adjusted to the robot morphology, and granular to sustain attention in long-term interaction. Most importantly, it needs to be targeted, in the sense that the robot must be able to chose particular classes of emotions for different situations. In this work, we implemented a Conditional Variational Autoencoder (CVAE), a deep learning framework, to learn a latent, low-dimensional probabilistic representation of EBL animations for a Pepper robot. The model was trained with a small set of hand-designed expressions and its latent space can be sampled to generate numerous new animations of targeted valence and arousal. We present the extensive results of a user study designed to evaluate the interpretability of the generated animations, how they compare with designed animations in terms of anthropomorphism and animacy, and to what extent they are considered as emotional and they draw users’ attention.

The paper is organized as follows: Section 2 briefly discusses related work and Section 3 describes the theoretical aspects of the CVAE. In Section 4 we outline the methodologies we used for structuring the training set and sampling the CVAE, and we describe the design of the user study and the statistical methods for the data analysis. The results are presented in Section 5.

2 Related work

Robotic EBL design has attracted much attention in recent years since for many robots, body motion is the main channel of non-linguistic expression. Nonetheless, comparing the proposed methodologies can be challenging due to differences in the design principles, the robot’s level of embodiment, the modalities involved in the expressions, the type of the expressions (static postures or dynamic animations), and the evaluation methodologies. Another important aspect of variability is the emotion representation model adopted by the researchers both in the development and the evaluation phase of the synthetic EBL expressions. The most broadly used model is the categorical representation, which is based on the discrete basic emotions theories. According to it, there is a core set of distinct emotion categories, the basic emotions, each corresponding to distinct brain locations or networks, each manifesting with a specific feeling and neuro-physiological signature [28]. Proponents of the theory maintain that this multimodular emotion system is universal within the human species and perhaps also shared by other primates [29, 30]. They also consider the basic emotions as prewired responses to different stimuli, an “affect program” written by the evolutionary process through natural selection, that can be however somewhat influenced epigenetically by learning. Arguably, the most frequently used emotion categories in the robotic EBL research is Ekman’s list of six basic emotions: anger, disgust, fear, happiness, sadness and surprise [31].

Another popular emotion representation in robotic EBL research is based on the dimensional models of emotion, in which affect states are represented by one or more continuous dimensions, each delimited by two polar states, such as pleased-displeased for the dimension of valence, activated-deactivated for the dimension of arousal, dominant-submissive for the dimension of control, approach-avoidance for the dimension of motivation. The most broadly adopted dimensional model is the *circumplex model of emotion* [32, 33], implemented as a two-dimensional space defined by the valence dimension ranging on a continuum from pleasure to displeasure on the horizontal axis, and the dimension of arousal ranging from activation to deactivation on the vertical axis. Russel and Barrett [32] suggest that these two affective dimensions may be sufficient to capture the core affect, which becomes a full-blown emotion when it is assessed within a situational framework. This representation allows us to depict core affect as a data point on this 2D space, which is visually intuitive and readily informative, and makes clear how different emotions are not independent from each other, but instead, they are variations of the same two variables. Another popular dimensional model is the PAD emotional state model [34], which uses an additional dimension, dominance, to support more nuanced emotions,

and discern states like anger and fear which are both of low valence and high arousal (i.e., fear is presumably of low dominance, while anger is of high).

In the following brief review, we summarize related work in robotic EBL synthesis under four main approaches: 1) Direct human imitation, 2) Feature-based design, 3) Creative design, and 4) Deep learning generative models. In many cases, researchers fuse elements from more than one approaches. The rest of this section discusses briefly each approach and provides some characteristic examples with a main focus on methods applied on humanoid robots and studies that include a user evaluation in terms of emotion recognition. For a broader systematic review on robotic animation techniques, the interested reader is directed to Schulz et al. [35].

2.1 Direct human imitation

In the first approach, the robot joints are configured to match the human joints in a single posture or motion setting. To accomplish this, computer vision techniques, markers, or sensors are employed to track key joint positions in human body motion, and then map them to the robot joint space manually by observation [36, 37, 38], or by way of a transfer function [39]. Regarding the second method, although it has an advantage as an end-to-end process, constructing good transfer functions can be very challenging because of the extensive differences in the morphology and kinematics. To the best of our knowledge, there are no studies so far applying it specifically for robotic EBL synthesis.

2.2 Feature-based design

A prominent approach in robotic EBL design is to use features extracted from human EBL. Such features can be found in studies coding postures or patterns of movement from recordings of actors performing emotional expressions [40, 41, 14, 42, 43, 44], computer-generated mannequin figures [8], or human motion capture data [45]. These studies provide lists of validated features, such as body orientation, the symmetry of limbs, joint positions, force, velocity, which can be employed for the design of robotic EBL expressions.

Regarding the emotion representation in humanoid robots, most of the studies use the categorical model (e.g., Ekman’s basic emotions) to design their robotic EBL expressions [46, 47, 48, 49, 50, 51], but some adopted the dimensional representation in the evaluation [46]. The robotic platforms used in these studies were Nao [46, 48], Daryl [47], Pepper and Hobbit [49], Brian 2.0 [50], and WABIAN-2R [52]. In the evaluation, some of the studies displayed the designed expressions on a physical robot [46, 47], while others on a virtual robot, videos or images of the physical robot [48, 50, 52]. The evaluation results in these studies vary a lot, something that comes as no surprise considering the differences in the platforms and the design principles. Häring et al. [46] found that all the body movements were rated in the right octant of the PAD model except *sadness* which was rated with positive arousal. Embgen et al. [47] reported that participants were able to identify the emotions from the EBL and Erden [48] that *anger* was recognized with 45%, *happiness* with 72.5%, and *sadness* with 62.5%. Tsiourti et al. [49] found that *happiness* was recognized more accurately, while *sadness* and *surprise* were poorly recognized from body motion alone. McColl and Nezat [50] found that *sadness* and *surprise* had the highest recognition rate (> 80%), while *fear* and *happiness* had the lowest recognition rate (< 30%). Destephe et al. [52] reported a high recognition rate for all the emotions (72.32% average).

Another feature-based paradigm for robotic EBL design is inspired by the Laban Motion framework [53], based on kinesiology, anatomy, and psychological analysis of human motion. Often, researchers use only a subset of the framework, the Laban Effort System, which provides four motion parameters: space, weight, time, and flow. These parameters have been used to handcraft features and generate locomotion trajectories that express affect in non-humanoid robots with low degrees of freedom [54, 55, 56, 57, 58], with promising results in terms of readability by humans. For example, Sharma et al. [55] used the four parameters to configure a set of flying patterns for a Parrot AR.Drone, and they found in their dimensional evaluation that space and time were significant predictors of valence, while all four Laban parameters could predict arousal. Takahashi et al. [58] designed expressions to convey the six basic emotions for a teddy bear robot using the Laban principles and they reported that although *fear* and *disgust* had a low recognition rate, the rest of the emotions were well recognised. The Laban Motion framework has also been used to design EBL for humanoids [59, 60, 61, 62, 63]. Masuda et al. [59] used Laban features (space, time, weight, inclination, height, area) to modify three basic movements for the humanoid robot HFR to express emotion. They found that *sadness* had the highest modulating effect.

Another interesting approach is to extract features from other human signals, such as voice, and encode them into robotic motion. The SIRE model [64] was proposed for generating robotic EBL based on four voice features: speed, intensity, regularity and extent. The model was evaluated on a Nao robot using the dimensional PAD model, and the results showed successful recognition of *happiness* and *sadness*.

Feature-based design can also be inspired by animal models instead of human EBL, an approach which can be potentially more effective with pet-like or animal-like robots [65]. Lakatos et al. [66] designed emotions of *fear* and *joy* for MogiRobi, a dog-like mechanical robot and they reported high recognition rates for *joy*. Other interesting studies on emotion modelling for animal-like robots include the seal-robot Paro [67, 68], the dog-robot AIBO [69], the cat-robot NeCoRo [70]. Although these studies have not directly evaluated emotion recognition and interpretability, they provide some indirect evaluation by testing the effects of using these emotionally expressive robots on robot-assisted therapy.

2.3 Creative design

Another influential approach in the design of robotic EBL emerges from applying the artistic principles and practices used in cartoon animation. The animator, conceives several expressive key postures for a given robot morphology, configures the robot like a puppet according to these postures to record the joints' positions, and then interpolates to derive intermediary positions so that the overall sequence appears continuous and smooth. This is the pose-to-pose animation technique. The approach is more robot-centric, in the sense that human EBL is not a direct prototype, and is often influenced by Disney's twelve basic principles of animation [71] producing very lifelike expressions. In some studies, puppeteers [72, 73] or random participants [74, 75] are enlisted to configure robot EBL postures or sequences of postures according to their subjective perception.

Monceaux et al. [76] describe their methodology of creating a big library of dynamic multimodal emotion expressions as an iterative process involving imitation from direct observation, and abstraction of key positions to adjust them to the Nao robot morphology. Ribeiro and Paiva [77] adapted Disney's twelve basic principles of animation [71] for an EMYS head robot to express the six basic emotions, on three different intensities. Their user study evaluation found that *anger*, *sadness* and *fear* were very well recognized. The principles of animation have also been used to design affect expression for non-humanoid robots. Yohanan and MacLean [78] followed a pose-to-pose design for the Haptic Creature, an animal-like robot. The modalities involved ears, lungs and purr and the dimensional representation was adopted both in the design and the evaluation. The design was found effective in conveying arousal but ambiguous in the communication of valence.

2.4 Deep learning approaches

Lately, there have been some efforts to generate robotic EBL using deep learning. Suguitan et al. [79] used human EBL for training three CycleGANs to generate animations expressing *happiness*, *sadness*, and *anger* for a Blossom robot with four degrees-of-freedom. They reported that the intended emotions were fairly discernible. Marmpena et al. [80] trained a Variational Autoencoder (VAE) with a small set of robotic EBL animations created from professional animators for a Pepper robot to generate numerous new ones. The model was agnostic to the emotion class of the EBL, but after inspecting how the sampled trajectories from the learned 3D spherical latent space are decoded to the robot's joints' space, the authors propose that the latent space radius can be used as a sampling parameter to modulate the arousal content of the generated animations. Suguitan et al. [81] also proposed a Variational Autoencoder, but they coupled it with a classifier to map the latent space motion representations to an emotion class. Their setup allows to modify a movement's emotion class by using latent space arithmetic. The user evaluation study showed that to some extent the modified movements are comparable to the original in terms of recognizability and legibility.

2.5 Contribution

Previous research has been mainly focused on hand-coded methods which can be tedious and expensive, thus resulting in a limited number of expressions, characterised by less granularity in their expressivity. Consequently, the expressions might appear repetitive and predictable which might be disengaging in long-term human-robot interaction. Furthermore, many of the previous studies used human EBL as a prototype, but scaling down the human motion range or excluding joints to match the robot's simpler morphology might end up losing information, or preserving redundant or trivial information with a negative impact on the lifelikeness of the robot character.

Our current work proposes a data-driven deep learning methodology for the automatic generation of numerous new robotic EBL animations, which appear smooth, natural, and exhibit increased granularity. Instead of human EBL, the prototype used is based on creative design which is directly adapted to the robot morphology and kinematics to ensure the illusion of life effect. Importantly, the proposed methodology seeks to generate animations of specific emotion class, so that the robot can select appropriate responses to given signals. Our work also seeks to leverage the dimensional representation of emotion, and more specifically the circumplex model of core affect [32, 33] with the dimensions of valence and arousal. We use the representation as an integral component of the generative process.

Concretely, we build on the methodology proposed in [80], where a VAE model was trained with a small set of hand-designed motion animations which were created with direct adaptation to the Pepper robot morphology and

motion capabilities. From the same work, we adopt the proposed method to modulate arousal by exploiting the geometry of the model’s latent space. For valence, we expand the VAE model to a conditional VAE (CVAE) which takes as input a label of valence as a continuous scalar value, and learns to adapt the generated animations based on it. Furthermore, to improve the expressiveness of the generated animations, we augmented the motion training set with sequences of eye LEDs’ colourful patterns.

3 Conditional Variational Autoencoders

The Variational Autoencoder (VAE) framework [82, 83, 84] can be used to learn a posterior probability distribution that represents the unknown underlying process that generates the observed data. Subsequently, this distribution can be sampled to generate purely novel content which is similar to the original. The VAE is composed of an encoder and a decoder, which can be implemented with any neural network architecture. During training, the vectorized input \mathbf{x} is passed through the encoder which compresses it into a lower-dimension stochastic representation \mathbf{z} , which retains all the sufficient information for a faithful reconstruction of \mathbf{x} . The distribution of all \mathbf{z} encodings defines a latent space, i.e., a continuous and structured manifold in which similar datapoints are close to each other. Then, the encoding \mathbf{z} is passed through the decoder which uses the information compressed in it to reconstruct the input.

In probabilistic graphical model formulation, the encoder is an inference model $q_\phi(\mathbf{z} | \mathbf{x})$ which approximates the true but intractable posterior. It infers the parameters of a predefined distribution, that is $\boldsymbol{\mu}$ and $\boldsymbol{\sigma}$ in the case of a multivariate Gaussian with a diagonal covariance matrix, which is the usual choice for real-valued output. Subsequently, the parameters are used to sample a latent datapoint \mathbf{z} , which is then passed through the decoder, a generative model $p_\theta(\mathbf{x} | \mathbf{z})$. Both ϕ and θ , the parameters of the two models, are learned jointly during training. This is accomplished by minimizing the following loss function:

$$\mathcal{L}_{\theta, \phi}(\mathbf{x}) = \underbrace{-\mathbb{E}_{\mathbf{z} \sim q_\phi(\mathbf{z} | \mathbf{x})}[\log p_\theta(\mathbf{x} | \mathbf{z})]}_{\text{reconstruction error}} + \underbrace{D_{KL}[q_\phi(\mathbf{z} | \mathbf{x}) || p_\theta(\mathbf{z})]}_{\text{regularization term}}, \quad (1)$$

In Eq. 1, the reconstruction error is the negative expectation of the log-likelihood taken over the latent parameters \mathbf{z} . It encourages the \mathbf{z} values that contribute to the faithful reconstruction of \mathbf{x} by the generative model. The regularization term (also called variational loss) is the Kullback-Leibler divergence which estimates the disparity between the latent distribution and a prior which is usually set to be a centered isotropic multivariate Gaussian. It incentivizes the inference model to learn \mathbf{z} values that are close to the prior distribution, and this way it applies a constraint on the latent space structure, resulting in a continuous manifold from which we can sample and generate new realistic samples.

The VAE is a powerful generative model, but in its standard form, there is no control on the class of the generated output. Controlling the generative process so that the decoded output matches a given class can be very important in certain applications. For example, in the present work, we want to be able to generate animations of targeted valence. The Conditional Variational Autoencoder (CVAE) [85], an extension of the VAE framework, does exactly what we need by learning to make a discriminative prediction additionally to reconstructing the input. This is accomplished by using an auxiliary variable \mathbf{c} , essentially a continuous or discrete label, to condition the encoding and decoding processes. The loss function of the CVAE modifies Eq. 1 as follows:

$$\mathcal{L}_{\theta, \phi}(\mathbf{x}, \mathbf{c}) = -\mathbb{E}_{\mathbf{z} \sim q_\phi(\mathbf{z} | \mathbf{x}, \mathbf{c})}[\log p_\theta(\mathbf{x} | \mathbf{z}, \mathbf{c})] + D_{KL}[q_\phi(\mathbf{z} | \mathbf{x}, \mathbf{c}) || p_\theta(\mathbf{z})]. \quad (2)$$

Fig. 1, illustrates the structure and computational flow of the CVAE. During training, at each step, we concatenate the input \mathbf{x} and the label \mathbf{c} , and we feed them as one vector to the encoder. The output of the encoder is reparameterized with some random noise ϵ to produce \mathbf{z} , which is concatenated with \mathbf{c} again and fed to the decoder, which outputs the reconstructed \mathbf{x} . After training, generating new output with label \mathbf{c} is accomplished by sampling a \mathbf{z} from the multivariate Gaussian prior, concatenation with \mathbf{c} and decoding.

4 Methods and materials

This section presents the training dataset and the implementation of the CVAE framework for robotic EBL generation, as well as the design of a user evaluation study and the statistical methods applied for the analysis of the collected data.

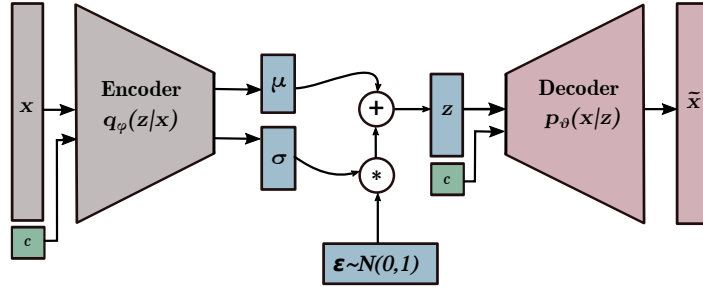


Figure 1: The structure and computational flow of the CVAE. Compared to the standard VAE, there is an additional input c (green block) that holds a label or an attribute on which we want to condition the generative process.

4.1 Training dataset

The dataset we used contains 36 robotic animations designed with the pose-to-pose method by professional animators for the Pepper robot. Initially, each animation consisted of three different modalities: motion, eye LEDs colour patterns, and non-linguistic sounds. Motion is represented by a series of keyframes, with each keyframe describing a posture defined by 17 values, i.e., the angles of the robot’s joints in radians (Fig. 2A). Each keyframe also has a timestamp indicating after how many frames (starting from 0) the posture should be executed. At runtime, the intermediary frame postures are obtained with cubic Bezier interpolation applied locally at each joint. The eye LEDs sequences are somewhat different in that their values can be set at any frame for a specified interval and they remain static until the interval is over. Pepper has two eyes with 8 LEDs each (Fig. 2B). Each LED is described by 3 values representing an RGB colour. Thus, in total, there are 48 LED values within a range of $[0, 1]$. For the current study, we excluded the audio modality.

The particular set of animations has been previously annotated with valence and arousal ratings in a user study with 20 participants [86]. In the present study, we only use the valence ratings as labels to condition the CVAE as described in Subsection 3. Each animation is annotated with a single real-valued label of valence in $[0, 1]$, where 0 indicates very negative valence and 1 very positive. For arousal, we used a different method of conditioning, based on the topology of the latent space (more details are provided in the next subsection).

Our goal for the CVAE training was to use postures as input at each timestep to allow the network to learn a continuous and structured manifold of postures, which can be interpolated to generate smooth sequences of motion. The initial keyframe representation was unsuitable for that, due to the abrupt changes between subsequent keyframe postures, and also the small size of the dataset. Furthermore, since the eye LEDs changes did not have the same onset with the keyframe postures, a dataset with the initial representation would be very sparse. To address these issues, we had the animations executed by the real robot and we recorded the angles of the joints and the eye LEDs values at a constant sampling rate of 25 frames per second, thus capturing both keyframes and intermediary frames. Before the recording, we made a small modification in the keyframe representation by adding an extra keyframe describing the StandInit posture (see posture in Fig. 2) at the beginning and the end of each animation (whenever it was missing), to obtain a clear onset and offset of an animation. In total, the initial keyframe representation dataset contained 697 keyframes, and with the recording we obtained 5074 frames. At this stage, each frame was a vector of 65 values: 17 values for the angles of the joints and 48 for the eye LEDs state.

The next issue to address was related to the prevalence of possible body orientations. For example, if many postures assume a right-side orientation, the training could be heavily biased and the network might not learn enough postures with left side orientation. We made the assumption that the interpretation of the bodily expression of emotion is independent of left or right side orientation with respect to the body’s vertical axis. This assumption allowed us to augment the dataset by having every posture mirrored from left to right or the opposite. We avoided any mirroring with respect to the horizontal axis of the body, e.g., changing upward motion to downward or vice versa, since such bias could affect the emotion content interpretation. More specifically, to create a mirrored posture we swapped the values of the entire chain of arm joints between the left and right arm, i.e shoulder pitch and roll, elbow roll and yaw, wrist yaw, and hand. For the roll and yaw joints of the arm, we had to additionally invert the signs of their values because the ranges of these joints had inverse signs between left and right. Furthermore, we also mirrored the head yaw and hip roll joints since these also move right and left with respect to the vertical axis of the body. For this mirroring, only the signs needed to be inverted. This augmentation doubled the dataset to 10148 frames.

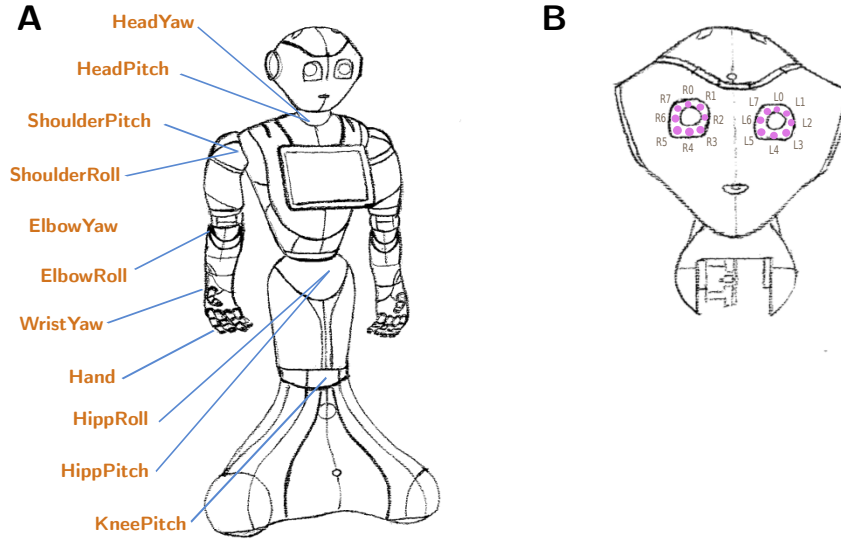


Figure 2: A) A Pepper robot has 17 joints that control the body configuration. The drawing shows the StandInit posture. B) The eye LEDs of Pepper. The robot has 8 RGB LEDs around each eye.

Regarding the valence attribute, we repeated the valence rating related to each animation for all the frames belonging to it. Therefore, each training example consists of 66 elements: 17 for the joints’ angles describing the posture, 48 for the eye LEDs state, and one value indicating the valence rating of the animation to which the frame belongs.

The last step in the preprocessing pipeline was the data normalization. The ranges of plausible joint values differ among the joints, thus we rescaled all the values in $[0, 1]$ with Min-Max Normalization. This was not necessary for the LEDs or the valence label since their range was already in $[0, 1]$. Since the implemented CVAE is agnostic to sequential dynamics of the dataset, we shuffled the dataset and used 80% for the training, and the rest for the validation.

4.2 CVAE network implementation

The CVAE framework for robotic EBL generation was implemented with Multilayer Perceptrons (MLPs). The decoder MLP has three dense layers with 128, 512, and 128 units respectively, as well as an additional dense layer after the output, serving as a reconstruction layer, with 66 units to match the input dimensions. The capacity of the encoder was increased by one extra fully-connected hidden layer with 512 units. This was decided after several empirical tests that showed that this configuration was more efficient to avoid posterior collapse¹. After each hidden layer, we used a layer of rectified linear activation functions (ReLU), while the output layers were followed by linear activations. The reconstruction layer of the decoder uses a sigmoid function to rescale the output in the range $[0, 1]$. After each hidden layer, we used a dropout layer, which randomly sets half of the units to zero [87]. This was not necessary in terms of regularization, but it improved the speed of the training.

For the latent layer, we used a strong bottleneck with only 3 dimensions. More dimensions did not decrease the validation error significantly, while less dimensions increased it. As we discussed in Section 3, the latent layer infers the parameters of a multivariate Gaussian distribution (a 3D Gaussian in our case), so it consists of two sub-layers of 3 units each, one for the latent mean μ and another one for the latent standard deviation σ used in the diagonal covariance matrix. In terms of the loss function implementation, the reconstruction error is equivalent to the Mean Squared Error (MSE) between the input and the reconstructed output when we assume a Gaussian model with real-valued output for the decoder. The regularization term can be computed analytically when we assume Gaussian distributions for both

¹Posterior collapse is a well documented problem arising in VAE training. It appears when the the model instead of learning meaningful latent features from the input, learns to ignore the latent variables resulting in a posterior distribution that collapses to the prior (usually selected to be an uninformative prior, e.g., a unit Gaussian). More concretely, posterior collapse indicates that the training is trapped into a trivial local optimum where $q_\phi(\mathbf{z} | \mathbf{x}) \simeq p(\mathbf{z})$ for all \mathbf{x} . Empirically, the problem can be detected during training when the variational loss $D_{KL}[q_\phi(\mathbf{z} | \mathbf{x}) || p_\theta(\mathbf{z})]$ becomes almost zero.

the prior and the approximate posterior [82]. Furthermore, the regularization term was weighted with a β coefficient [88, 89]. In general, the larger this hyperparameter is, the stronger the pressure on the approximate posterior $q_\phi(\mathbf{z} | \mathbf{x})$ to match the prior $p_\theta(\mathbf{z})$. However, a large β might also have a cost on the reconstruction fidelity. After several empirical tests, we tuned the hyperparameter to $\beta = 0.001$. This value was found to allow a low reconstruction error and also a well structured latent space.

The network weights were initialized with a Xavier uniform initializer [90], i.e., the initial weight of each unit was sampled from a uniform distribution with limits normalized by the sum of its input and output units. For the optimization, we used an Adam optimizer [91] with a learning rate set to $1e-4$. Finally, we trained for 250 epochs.

4.3 Conditional sampling of the latent space

The simplest way to generate a new animation with the trained CVAE is to randomly sample the prior distribution (centered isotropic 3D Gaussian) as a proxy for the learned latent space, interpolate the samples, concatenate the target valence label at each datapoint, and finally decode them into the joint space. However, a more systematic sampling method proposed in previous work [80] uses concentric spherical grids projected conceptually on the latent distribution and samples latent trajectories along their longitudes. This work showed that trajectories sampled from the inner spheres, closer to the core (which is also the center of the latent zero-centered distribution), decode into animations with lower amplitude and variance compared to animations decoded from trajectories sampled from the outer spheres. Based on this finding, it was suggested that the radius of the projected spheres can be used as a topological feature that modulates the arousal content of a generated animation. Therefore, to generate low arousal animations, we use a small radius as standard deviation to sample the prior distribution, and when we want to increase the arousal we increase the radius.

In the current work, we test this hypothesis about the arousal conditioning but we modify the conceptual tool of the spherical grid into a torus. A shortcoming of the spheres was that the decoded animations appeared to begin and end abruptly, and always in the same robotic posture. This is due to the fact that all the longitudes of a sphere end at the same point, the pole of the sphere. Especially in larger spheres, this point is far away from the origin where all three latent dimensions (LD1, LD2, LD3) are equal to zero, i.e., the encoding that decodes into the StandInit position, the most neutral and symmetric posture. By changing the spherical grid topology into a torus grid, and more specifically, a *horn torus* (see Fig. 3), which is a torus without a hole, with all the circles forming its tube touching each other at the centre of the 3D latent space where $LD1 = LD2 = LD3 = 0$, we get a clear advantage. Although all the longitudinal trajectories begin and end at the same point, and unlike the poles of the sphere, this point is now located in the core of the latent space, and thus, it decodes into the StandInit posture. This way, we obtain a clear onset and offset of the animation and we still keep the radius feature with which we will modulate the arousal dimension of the generated animations.

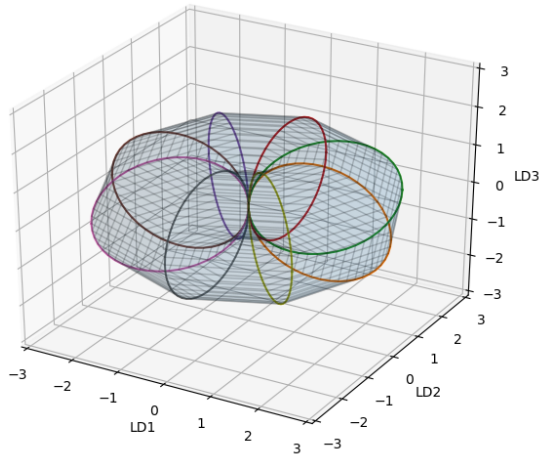


Figure 3: An example of a horn torus grid used as a template for the systematic sampling of latent trajectories. In this example, the radius is equal to 3, and the axis is in parallel with the latent dimension LD3. All torus grids have their center in the core of the latent space where $LD1 = LD2 = LD3 = 0$. The latent trajectories are sampled along the colored longitude lines.

To condition the generated animations on the arousal as hypothesized to be modulated by the radius of the latent space, we defined three levels of arousal (low, medium, and high), which were obtained by sampling the 3D latent space with a radius of 3, 4, and 5 respectively. More concretely, we sampled 8 circular latent trajectories from torus grids rotated in three ways (so that the central axis is parallel to one of three latent dimensions), and radiuses of 3, 4 and 5. For example, Fig. 3 illustrates 8 circular trajectories from a torus grid of radius equal to 3, and its central axis in parallel with LD3. Note that in this approach we define radius as the distance from the centre of the latent space to the outer point of the torus surface as if the whole torus is enclosed in a sphere with the same centre. Each latent circle was defined by 20 points. Subsequently, the 20 points of each latent trajectory were interpolated using B-spline interpolation of 15, 20, 25 steps per segment for radius 3, 4, and 5 respectively. We gradually increased the interpolation steps as the radius increased to keep similar distances between the points of each interpolant. In total, we derived 72 latent trajectories (8 longitudes * 3 radius values * 3 latent dimensions) with 20 points each.

Subsequently, to condition the generative process with the valence label, we concatenated each of the 72 latent interpolants with 3 different values representing levels of valence: 0 for negative, 0.5 for neutral, and 1 for positive. Thus we obtain 216 latent trajectories which were passed through the decoder of the CVAE to get the final library of 216 generated animations. Essentially, the valence conditioning is achieved via the CVAE model structure, while the arousal conditioning is accomplished explicitly based on the topological features of the spherical latent space.

4.4 Evaluation study

This section presents the design of a user study aimed to evaluate the interpretability of the CVAE generated animations with respect to the valence and arousal conditioning. The statistical methods applied for the analysis of the collected data are also presented.

4.4.1 Participant’s profile

A total of 20 volunteers were recruited for this study (9 female and 11 male). The mean age was 26.4 years ($SD = 5.36$, $min = 21$, $max = 44$). All participants were employees of SoftBank Robotics Europe, in various professional roles, e.g., engineers, administrative staff, marketing, etc. They self-reported their experience with the robot’s animation capabilities on a scale ranging from 0 (no experience at all) to 10 (extremely familiar). The mean self-reported experience was equal to 6.35 ($SD = 1.81$, $min = 3$, $max = 9$). The experiment was carried out at the company’s premises in Paris, France. The experimental protocol was granted ethical approval by the University of Plymouth, Faculty of Science and Engineering Research Ethics Committee.

4.4.2 General setup

The experimenter briefly explained that the aim of this experiment was to evaluate a set of body language animations displayed by Pepper. This would require to observe the robot located in front of the participant, approximately 2.5 meters away, and reply to the questions appearing on a screen right in front of the participant. The session was split into three parts, all of which were completed by each participant. In general, when deciding on the number of trials, as well as the length of questionnaires, our main concern was to keep participant’s workload as low as possible, so that they could retain their concentration and motivation. The interface was implemented as a website running on a local server and it was projected on the screen. The participant would click on a play button to give the command for the robot to execute an animation, and afterwards, at her own pace, she would insert her responses.

4.4.3 Stimulus, interface, and questionnaires

The stimuli used for this experiment were animations displayed on a physical Pepper robot. More specifically, we had two kinds of animations: *designed* animations, designed by professional animators with the pose-to-pose method, and *generated* animations, generated with the CVAE and the sampling method we described in section 4.3.

Part A: This part aimed to compare the *designed* animations to the *generated* ones in terms of the anthropomorphism and animacy degree attributed to the robot. It consisted of two trials, in which participants watched the robot executing 9 *designed*, and 9 *generated* animations. In both groups, the animations were displayed continuously without a pause. The animations were randomly selected in each group from the respective broader libraries of *designed* and *generated* animations. The two trials appeared in randomized order. After each trial, participants had to fill in a questionnaire comprised of two scales, Anthropomorphism and Animacy, selected from the Godspeed Questionnaire Series (GQS) [92]. Anthropomorphism is a measure of how humanlike the robot appears to be. The scale comprises of five 5-point semantic differentials (Fake/Natural, Machinelike/Humanlike, Unconscious/Conscious, Artificial/Lifelike, and Moving rigidly/Moving elegantly). Animacy is a measure of how lifelike the robot appears to be. The scale comprises of six

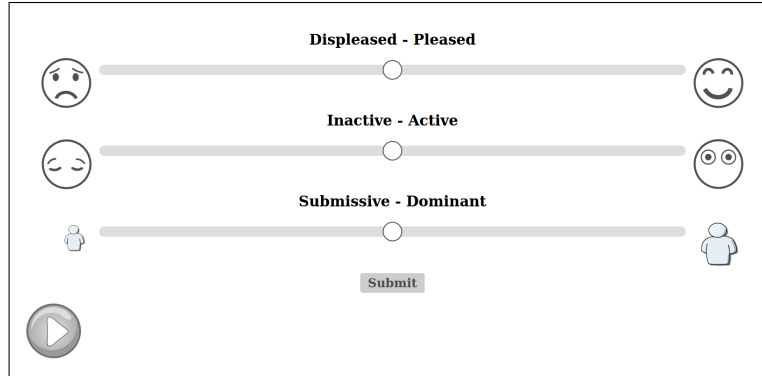


Figure 4: The view we used to collect valence, arousal and dominance ratings. The participant clicks on the play button and watches the real robot executing a generated animation. Subsequently, the user clicks on the three sliders to enter the perceived valence, arousal and dominance scores. The concept is adopted from the Affective Slider [93].

5-point semantic differentials (Dead/Alive, Stagnant/Lively, Mechanical/Organic, Artificial/Lifelike, Inert/Interactive, Apathetic/Responsive).

Part B: This part involved only *generated* animations, which were evaluated on three dimensions of emotion: valence, arousal and dominance. It consisted of 18 randomized trials. In each trial, a single *generated* animation was displayed on the robot when the participant clicked on a digital play button. After the animation was over, the participant would enter the dimensional ratings on three different sliders as depicted in Fig. 4. The sliders were titled with the two extremes of each measured emotion dimension: for valence the title is *Displeased - Pleased*, for arousal *Inactive - Active*, and for dominance *Submissive - Dominant*. We selected this verbal description as more intuitive. The interface uses visual aids to illustrate the extremes in a more intuitive way. The whole idea of this view is based on the Affective Slider [93], a digital scale for the self-assessment of emotion, which we modified by adding the extra dimension of dominance (*Submissive - Dominant*) and also by making small changes to the original icons for valence and arousal to avoid misreadings between valence and arousal. The participants were allowed to click the play button and watch the animation for a second time if needed. After watching the animation they could click on the sliders to enter their ratings. Each slider was constructed with a range in $[0, 1]$ and 100 points of discretization. However, the numerical representation was hidden.

After submitting the ratings, a second view appeared in the same trial. It contained two 5-point Likert scales and the play button. The two declarations on the Likert scales were “The robot’s behaviour draws my attention” and “The robot’s expression was emotional”. The responses for each of declaration were: Strongly disagree, Disagree, Neither agree nor disagree, Agree, Strongly agree. The participant could watch the animation once more if it was necessary to recall it in the context of the new set of questions. The first Likert declaration is adapted from [94], a study that proposes several dimensions and related metrics to evaluate the believability of an artificial agent. The authors of this study, propose a Likert scale with the template phrase, “<X>’s behaviour draws my attention.” as a quantifiable metric of the *visual impact* dimension of believability. The second Likert scale was constructed by us as a manipulation check, to obtain a secondary, more direct and general assessment on whether participants perceived a *generated* animation as an emotional expression. The 18 *generated* animations used in Part B were selected randomly from the broader set of generated animations, obtained as we described in Section 4.3. We aimed to have 2 animations for each combination of valence and arousal levels. The task was solicited with the question ‘How does the robot feel?’. A practice period of 3 trials preceded it so that the participants could get accustomed to the use of the sliders and the emotion dimension concepts.

Part C: This part was identical to Part A in terms of structure but used different *designed* and *generated* animations to minimize the chances of confounds due to the choice of animations. Furthermore, the *generated* animations used in Part A and C were excluded. Part C, was added as a pretest-post-test design to examine if the results of the comparison between designed and generated samples (on anthropomorphism and animacy) persist or change after the participants become more familiar with the robot range of motion.

4.5 Statistical analysis

The statistical analysis of the collected data examines: 1) How valence and arousal conditioning of the generative process influences participants in their evaluation of the generated animations’ valence, arousal and dominance, 2) How

the participants compare the generated vs the hand-designed animations in terms of anthropomorphism and animacy, and 3) How valence and arousal conditioning of the generative process influences the participants’ attention and their belief that the animations express emotions.

4.5.1 Valence, arousal and dominance ratings

This analysis aims to explore how valence and arousal conditioning of the generated animations affected the ratings of valence, arousal and dominance assigned by the participants. Our two independent variables are the following: 1) v_cond with levels *negative*, *neutral*, and *positive* refers to the valence conditioning of the CVAE generative process using an attribute c equal to 0, 0.5, and 1 respectively, and 2) a_cond with levels *low*, *medium*, and *high* represents the arousal sampling of the CVAE’s latent space using a radius r equal to 3, 4, and 5 respectively.

There are three dependent variables, *valence*, *arousal* and *dominance*, which are based on the corresponding slider ratings given by the participants. Since we had multiple responses from a participant within the levels of the independent variables (e.g., a participant rated 6 animations with $v_cond = neutral$), we aggregated the ratings for each participant within each level of the two independent variables v_cond and a_cond . The aggregation was based on the mean within each level.

The main research question is whether the valence and arousal ratings given by the participants are affected by the valence and arousal conditioning we used to generate the animations. Specifically, we had two hypotheses:

- **H1:** Valence ratings for animations generated with $v_cond = negative$ will be lower than those of animations generated with $v_cond = neutral$ or $v_cond = positive$. Valence ratings for animations generated with $v_cond = neutral$ will be lower than those of animations generated with $v_cond = positive$.
- **H2:** Arousal ratings for animations generated with $a_cond = low$ will be lower than those of animations generated with $a_cond = medium$ or $a_cond = high$. Arousal ratings for animations generated with $a_cond = medium$ will be lower than those of animations generated with $a_cond = high$.

We also conducted an exploratory analysis to examine whether v_cond had an effect on the arousal or dominance ratings, and similarly, if a_cond had an effect on valence or dominance ratings. Since the experimental design was within-subjects, i.e., each participant evaluated animations in each level of the independent variables, we used repeated-measures one-way analysis of variance (ANOVA). The test was decided to be one-way (with a single independent variable at a time) because the data aggregation applied on the levels of each independent variable could not be applied concurrently for both independent variables without inflating the number of appearances of each animation and inserting multiple missing values. In total, we applied 6 such tests and we conducted post hoc comparisons between the levels of the independent variables with paired samples t-tests, only for those relationships that were found significant. The p values were adjusted with Bonferroni correction for multiple comparisons error. Before proceeding with the tests, we checked whether the necessary ANOVA assumptions hold. We checked for outliers using boxplot methods. The normality assumption was tested with the Shapiro-Wilk test and visual inspection of the QQ plots within each level of the independent variables. The assumption of sphericity was checked with Mauchly’s test and Greenhouse-Geisser sphericity correction was applied when the assumption was violated.

4.5.2 Comparison of designed and generated animations

This analysis aims to examine the comparison between generated and *designed* animations in terms of anthropomorphism and animacy. It also examines for possible effects arising from the pretest-posttest experimental design (Part A vs Part C as described in 4.4.3) to determine if the attribution of anthropomorphism and animacy is altered after the participants become more familiar with the robot’s body language. The main hypothesis for this analysis is the following:

- **H3:** The attribution of anthropomorphism and animacy to the robot is not significantly different between the *designed* and the *generated* animations, either in the pretest trials (Part A) or the posttest trials (Part C).

Initially, we computed Cronbach’s alpha to estimate the internal consistency of the responses as a measure of reliability. An acceptable reliability would permit to collapse the items of each scale to a single response per participant and per scale using a measure of central tendency. The decision was based on a threshold $\alpha > 0.7$ which is widely considered as an indication of acceptable internal consistency. Given that result, we proceeded with taking the median of the items of each scale and each participant, i.e., one score for Anthropomorphism and another one for Animacy for each participant. Since Likert scales provide ordinal data, the mean is not considered a valid parameter to aggregate their items, and similarly, parametric tests cannot be applied due to the normality assumption, thus we used ordered logistic regression [95] to model the effects. For pairwise differences of the estimated marginal medians, the p values of the contrasts were corrected with Tukey’s multiple comparisons adjustment.

Aggregated ratings	v_cond level	Mean	SD	a_cond level	Mean	SD
valence	Negative	0.46	0.12	Low	0.47	0.1
	Neutral	0.54	0.09	Medium	0.54	0.11
	Positive	0.57	0.12	High	0.55	0.13
arousal	Negative	0.55	0.12	Low	0.5	0.12
	Neutral	0.55	0.12	Medium	0.55	0.12
	Positive	0.58	0.11	High	0.63	0.14
dominance	Negative	0.4	0.12	Low	0.42	0.11
	Neutral	0.46	0.1	Medium	0.44	0.09
	Positive	0.52	0.13	High	0.52	0.12

Table 1: Summary statistics for valence, arousal and dominance ratings

We fitted 3 models for each scale. The first one aimed to predict the Likert scores using the group of the animation set (designed_pre, generated_pre, designed_post, generated_post) as a predictor, and to examine if there are differences between the *generated* and the *designed* animations, either in the pretest phase or the posttest, according to **H3**. For the second model, we used as a predictor only two groups (pre, post), each containing both designed and generated animations, in order to explore if there are pretest-posttest differences in general. The third model aimed to examine potential gender differences affecting the overall scores of anthropomorphism and animacy. Finally, we applied a likelihood ratio test to each model in order to test if the proportional odds assumption of the ordered logistic regression holds. This is a crucial assumption for ordinal regression analyses, and it asserts that the independent variables have the same effect on the odds irrespective of the splits between each pair of levels of the ordinal outcome variable. The null hypothesis of the test upholds the proportionality of the odds, thus for the assumption to be justifiable, it must not be rejected.

4.5.3 Attention and emotional content

This analysis examines the effect of the CVAE conditioning variables *v_cond* (levels Negative, Neutral, Positive) and *a_cond* (levels Low, Medium, High) on the 5-point Likert scores of two items: *Attention* (“The robot’s behaviour draws my attention”) and *Emotion* (“The robot’s expression was emotional”). For each of the Likert items, we fit an ordered logistic regression model and checked for pairwise differences with Tukey’s adjustment of *p* values. The proportional odds assumption is checked again with likelihood ratio tests.

4.6 Software

For recording and executing robotic animations with a Pepper robot we used NAOqi 2.5 SDK². For the robot simulations we used the Choregraphe Suite³. The code for the CVAE model was adapted from the TFModelLib collection of neural networks⁴. For the implementation of B-splines we used Splipy⁵. The rest of the code for the CVAE implementation (data preprocessing, sampling, torus grids, etc.) was written in Python 3 with packages such as NumPy [96], SciPy [97], pandas [98], scikit-learn [99], Matplotlib [100]. The interface for the user study data collection was written in Python 2 with Django v1.11.10⁶. The statistical analysis of the collected data was carried out in R [101, 102, 103, 104, 105, 106, 107, 108].

5 Results

5.1 Valence, arousal and dominance ratings

In Table 1, we present the descriptive statistics of the aggregated ratings (valence, arousal, and dominance), with respect to the levels of the explanatory variables *v_cond* and *a_cond*.

Regarding the normality assumption, only two extreme outliers were detected, one in the relationship where *v_cond* is used to predict arousal, and a second one where *a_cond* is used to predict valence. Since these relationships are not

²NAOqi 2.5: http://doc.aldebaran.com/2-5/home_pepper.html

³Choregraphe Suite 2.5: <http://doc.aldebaran.com/2-5/software/choregraphe/index.html>

⁴TFModelLib repository: <https://github.com/nhemion/tfmodellib>

⁵Splipy v1.3.1: <https://sintefmath.github.io/Splipy/>

⁶Django web framework: <https://www.djangoproject.com/>

DV	IV	Group 1	Group 2	t(df)	p	p (adjusted)
valence	v_cond	Negative	Neutral	$t(19) = -3.65$	0.002	0.005**
		Negative	Positive	$t(19) = -4.47$	< 0.001	< 0.001***
		Neutral	Positive	$t(19) = -1.63$	0.12	0.36
dominance	v_cond	Negative	Neutral	$t(19) = -2.06$	0.05	0.16
		Negative	Positive	$t(19) = -4.69$	< 0.001	< 0.001***
		Neutral	Positive	$t(19) = -3.46$	0.003	0.008**
arousal	a_cond	Low	Medium	$t(19) = -2.27$	0.04	0.11
		Low	High	$t(19) = -3.62$	0.002	0.005**
		Medium	High	$t(19) = -2.88$	0.01	0.029*
dominance	a_cond	Low	Medium	$t(19) = -0.89$	0.381	1
		Low	High	$t(19) = -4.37$	< 0.001	< 0.001***
		Medium	High	$t(19) = -5.24$	< 0.001	< 0.001***

Note: DV = Dependent Variable, IV = Independent Variable, t(df) = t statistic and degrees of freedom, p = p values, p (adjusted) = p values with Bonferroni correction.

Table 2: Post hoc tests for valence, arousal and dominance ratings

substantial for our main hypotheses and we only have an exploratory interest in them, we decided to proceed. All three dependent variables—valence, arousal and dominance—were found normally distributed at each level of v_cond as assessed by Shapiro-Wilk’s test ($p > 0.05$). The same was true for arousal and dominance with respect to the levels of a_cond , but valence was found to violate the assumption for the a_cond level *medium* ($p = 0.029$). Again, taking into account that it is not in our main hypothesis to predict valence ratings with the arousal conditioning of the CVAE, this violation of the normality assumption was not of concern. Furthermore, one-way ANOVA is considered a robust test against the normality assumption.

First, we will discuss the results for the tests in which we used the valence conditioning of the CVAE (v_cond), to predict valence, arousal and dominance ratings. The results revealed a significant effect of v_cond on the aggregated valence ratings ($F(2, 38) = 13.5$, $p < 0.001$, $\eta_g^2 = 0.16$) and on the aggregated dominance ratings ($F(2, 38) = 12.6$, $p < 0.001$, $\eta_g^2 = 0.16$). No significant effect was detected on arousal ($F(2, 38) = 1$, $p = 0.38$, $\eta_g^2 = 0.01$).

With regard to the arousal conditioning of the CVAE (a_cond), the one-way repeated-measures ANOVAs detected significant effects on the aggregated valence ratings ($F(2, 38) = 6.47$, $p = 0.004$, $\eta_g^2 = 0.09$), the aggregated arousal ratings ($F(1.5, 28.42) = 10.19$, $p = 0.001$, $\eta_g^2 = 0.15$, with Greenhouse-Geisser correction for the degrees of freedom due to sphericity assumption violation), and the aggregated dominance ratings ($F(2, 38) = 16.159$, $p < 0.0001$, $\eta_g^2 = 0.166$).

Pairwise differences between the levels of conditioning were examined with post hoc tests and are summarized in Table 2. We excluded the relationships for which ANOVAs did not reveal significant effects (arousal with v_cond as a predictor), and also those for which the normality assumption was violated (valence with a_cond as a predictor).

For the effect of v_cond on valence ratings (Fig. 5A), paired samples t-tests with Bonferroni correction revealed statistically significant differences for Negative-Neutral ($t = -3.65$, $p = 0.005$) and Negative-Positive ($t = -4.47$, $p < 0.001$). Thus, the results partially support the hypothesis **H1**, in that animations generated with negative valence conditioning received lower valence ratings compared to animations generated with neutral or positive valence conditioning.

For the effect of a_cond on the arousal ratings (Fig. 5B), paired samples t-tests with Bonferroni correction detected statistically significant differences for Low-High ($t = -3.62$, $p = 0.005$) and Medium-High ($t = -2.88$, $p = 0.029$). For Low-Medium a statistically significant difference was detected ($t = -2.27$, $p = 0.01$), but it did not survive the Bonferroni adjustment. Thus, the results partially support the hypothesis **H2**, in that animations generated with high arousal conditioning received higher arousal ratings compared to animations generated with low or medium arousal conditioning.

Furthermore, we conducted post hoc tests to examine the pairwise differences in the levels of v_cond and a_cond regarding their effect on the aggregated dominance ratings. For v_cond , statistically significant differences were detected for Negative-Positive ($t = -4.69$, $p < 0.001$) and Neutral-Positive ($t = -3.46$, $p = 0.008$) (Fig. 6A). For a_cond , statistically significant differences were detected for Low-High ($t = -4.37$, $p < 0.001$) and Medium-High ($t = -5.24$, $p < 0.001$) (Fig. 6B). These results suggest that the CVAE conditioning with v_cond and a_cond can

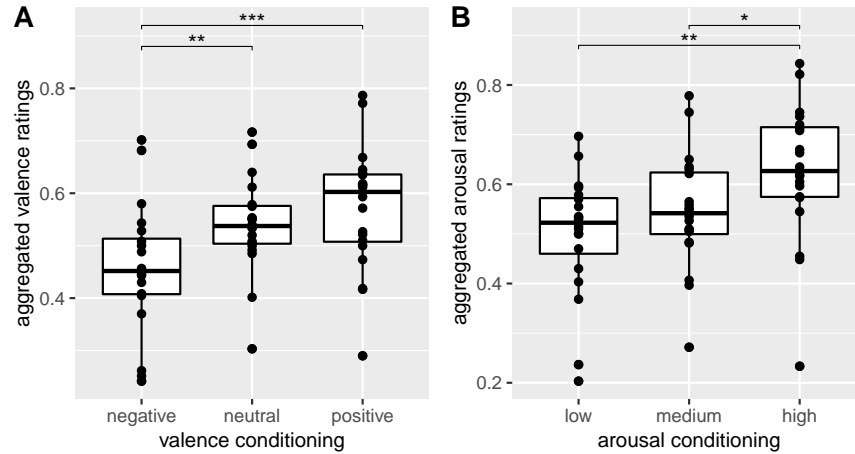


Figure 5: Post hoc t-tests with Bonferroni adjustment. A) Valence conditioning impact on valence ratings. B) Arousal conditioning impact on arousal ratings. The graph was originally published in [109]

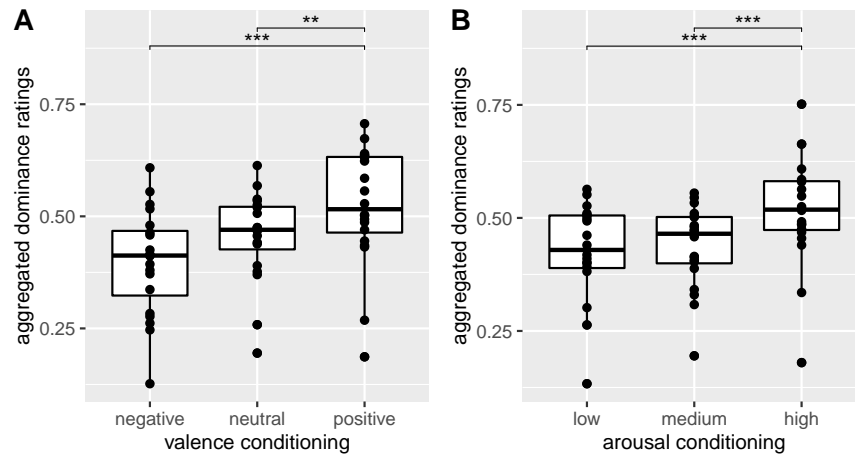


Figure 6: Post hoc t-tests with Bonferroni adjustment for multiple comparisons. A) Differences among the valence conditioning levels with respect to the participants' aggregated ratings of dominance. B) Differences among the arousal conditioning levels with respect to the participants' aggregated ratings of dominance.

potentially influence how people perceive the level of dominance in the robot's expression, with positive valence or high arousal conditioning making the robot to appear more dominant in terms of the simulated emotion.

5.2 Comparison of designed and generated animations

We begin the presentation of the results with the descriptive statistics presented as bar plots in Fig. 7 for the Anthropomorphism and Animacy scores. The responses are from 1 to 5 (with 5 indicating that the participant attributes a higher degree of Anthropomorphism or Animacy to the robot), and the percentages represent the portion of participants in each response. The basic contrast is *designed* vs *generated* animations presented in the pretest phase (Part A of the session) and then again in the posttest phase (Part C).

For each scale (Anthropomorphism and Animacy), the internal consistency tested with Cronbach's alpha was found above our chosen threshold $\alpha \leq 0.85$. Thus, we proceeded with collapsing the semantic differentials of each scale (5 items for Anthropomorphism and 6 for Animacy) in one score per participant and per group, by taking the median value.

DV	IV	Coef.	SE	t	p	95% CI
Anthropomorphism	generated_pre	-0.20	0.58	-0.35	0.730	(-1.34, 0.93)
	designed_post	0.57	0.58	0.98	0.328	(-0.57, 1.73)
	generated_post	0.46	0.57	0.81	0.420	(-0.66, 1.60)
Animacy	generated_pre	0.38	0.67	0.57	0.572	(-0.94, 1.71)
	designed_post	1.15	0.66	1.75	0.080	(-0.13, 2.46)
	generated_post	0.81	0.69	1.18	0.240	(-0.54, 2.19)
Anthropomorphism	posttest	0.61	0.41	1.49	0.135	(-0.19, 1.42)
Animacy	posttest	0.83	0.49	1.69	0.091	(-0.12, 1.81)
Anthropomorphism	Male	-0.86	0.42	-2.06	0.039*	(-1.69, -0.05)
Animacy	Male	-0.45	0.49	-0.92	0.359	(-1.42, 0.5)

Note: DV = Dependent Variable, IV = Independent Variable, Coef. = Coefficient of ordered logistic regression model, SE = Standard Error, t = t statistic, p = p value, CI = Confidence Interval.

Table 3: Ordered logistic regression results for Anthropomorphism and Animacy

In terms of the hypothesis **H3** testing with ordered logistic regression, none of the groups (designed_pre, generated_pre, designed_post, generated_post) was found to have a statistically significant effect for Anthropomorphism or Animacy (results are summarized in Table 3). This result supports our hypothesis that participants do not attribute different Anthropomorphism or Animacy levels to the *designed* animations compared to the *generated* ones, either in the pretest or posttest phase. In Fig. 8, we plot the probabilities derived from the predictions of the two ordered logit models of Anthropomorphism and Animacy scores for each group of animations.

The two models of ordered logistic regression for Anthropomorphism and Animacy with all the pretest and all the posttest animations as a two-level predictor revealed some trends for Animacy (Fig. 9B), but no significant effects were detected for either scale, suggesting that the interval in between the two evaluations did not impact significantly the perception of Anthropomorphism and Animacy. The detailed results are presented in Table 3.

Finally, regarding the two models that tested for gender effects, female participants gave higher scores than male ($p = 0.039$) on the Anthropomorphism scale, but no statistically significant differences were detected for Animacy ($p = 0.35$). The predictions' probabilities are plotted in Fig. 10 and the detailed results are included in Table 3.

The likelihood ratio tests checking for violations of the proportional odds assumption did not obtain statistically significant p values for any of the six models (all p values ≤ 0.08), thus the assumption was considered tenable.

5.3 Attention and emotional content

The descriptive statistics of the Attention and Emotion Likert scales with respect to the valence and arousal conditioning levels are presented in Fig. 11 as bar plots with the exact percentage for each response. The two ordered logistic regression models that predicted the Attention Likert scores (“The robot’s behaviour draws my attention”) with the valence and arousal conditioning of the CVAE as a predictor respectively, detected statistically significant effects. The results are summarised in Table 4.

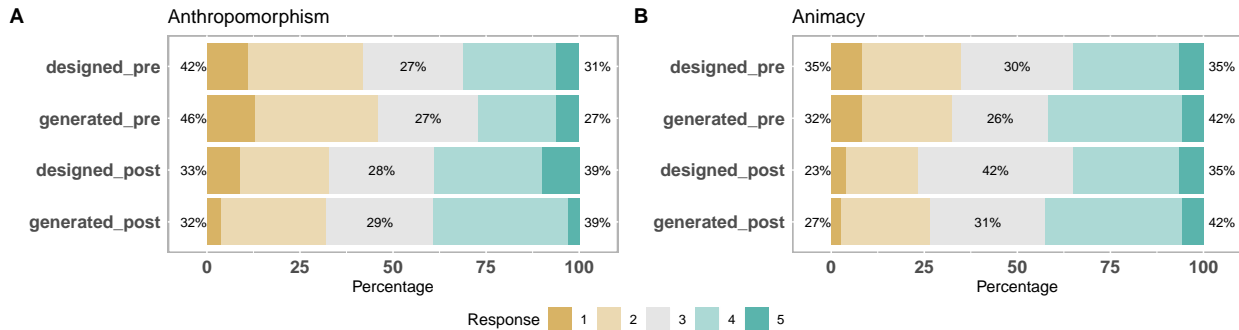


Figure 7: Anthropomorphism (A) and Animacy (B) bar plots for designed vs generated animations in pretest and posttest phase.

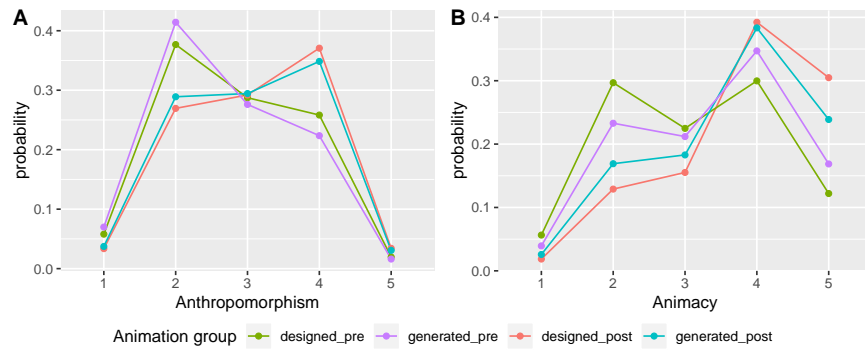


Figure 8: Anthropomorphism and Animacy scores for designed vs. generated animations. The *pre* and *post* suffixes indicate the evaluation that was conducted during Part A and Part C of the experimental session respectively.

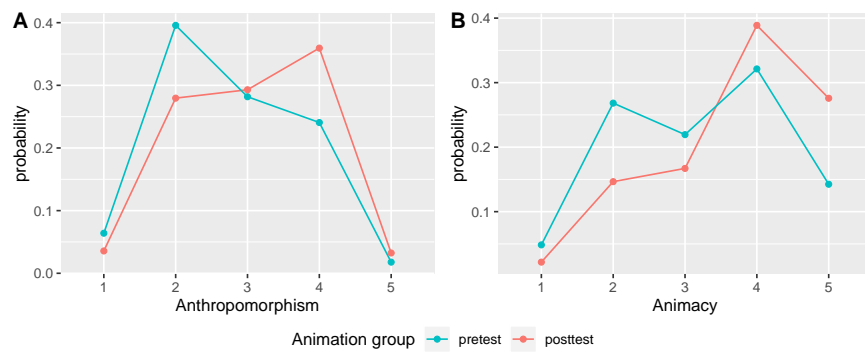


Figure 9: Anthropomorphism and Animacy scores for all the animations evaluated in Part A and Part C. A slight increase in the posttest phase, is not confirmed with statistically significant results in pairwise comparisons.

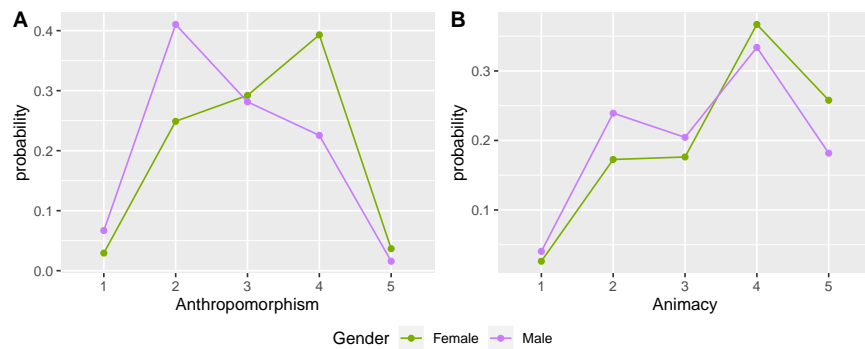


Figure 10: Anthropomorphism and Animacy scores between male and female participants. Female participants gave significantly higher Anthropomorphism ratings.

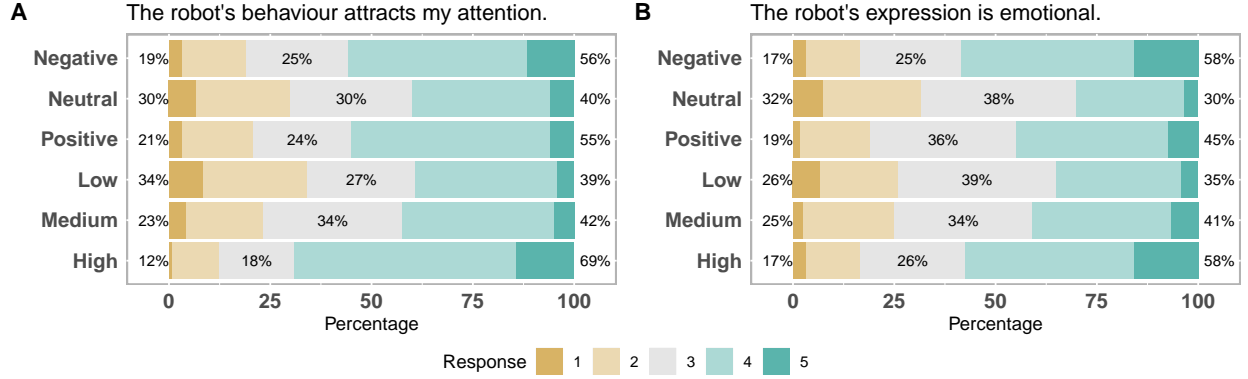


Figure 11: Bar plots for Attention and Emotion Likert scores with respect to the valence (Negative, Neutral, Positive) and arousal (Low, Medium, High) conditioning levels.

Post hoc tests on the levels of the valence conditioning (v_cond) determined that the contrast Negative-Neutral was statistically significant ($z = 2.77$, $p = 0.02$), suggesting that animations generated with negative valence conditioning might attract more attention from participants compared to animations generated with neutral valence. This result is illustrated in Fig. 12A, where we present the probabilities of predictions obtained by the model. In the same figure, we observe that the same appears to be true for animations generated with positive conditioning, however, this difference (Neutral-Positive) did not survive the Tukey adjustment of the p value. The results are summarized in Table 5.

DV	IV	Coef.	SE	t	p	95% CI
Attention	v_cond :Neutral	-0.11	0.17	-0.64	0.52	(-0.44, 0.22)
	v_cond :Negative	0.48	0.17	2.85	< 0.001***	(0.15, 0.81)
Attention	a_cond :Medium	0.95	0.18	5.33	< 0.001***	(0.60, 1.30)
	a_cond :High	0.29	0.17	1.73	0.08	(-0.04, 0.62)
Emotion	v_cond :Neutral	-0.36	0.17	-2.10	0.04*	(-0.69, -0.02)
	v_cond :Negative	0.74	0.17	4.39	< 0.001***	(0.41, 1.07)
Emotion	a_cond :Medium	0.63	0.17	3.71	< 0.001***	(0.30, 0.97)
	a_cond :High	0.19	0.17	1.18	0.24	(-0.13, 0.52)

Note: DV = Dependent Variable, IV = Independent Variable, Coef. = Coefficient of ordered logistic regression model, SE = Standard Error, $t = t$ statistic, $p = p$ value, CI = Confidence Interval.

Table 4: Ordered logistic regression results for Attention and Emotion

DV	IV	Group 1	Group 2	z	p (adjusted)
Attention	v_cond	Negative	Neutral	2.77	0.02*
		Negative	Positive	0.64	0.8
		Neutral	Positive	-2.16	0.08
Attention	a_cond	Low	Medium	-1.34	0.37
		Low	High	-5.33	< .001***
		Medium	High	-4.17	< .001***
Emotion	v_cond	Negative	Neutral	4.75	< .001***
		Negative	Positive	2.1	0.09
		Neutral	Positive	-2.81	0.01**
Emotion	a_cond	Low	Medium	-0.89	0.64
		Low	High	-3.71	< .001***
		Medium	High	-2.85	0.01**

Note: DV = Dependent Variable, IV = Independent Variable, $z = z$ statistic, p (adjusted) = p value with Tukey correction

Table 5: Post hoc tests for Attention and Emotion

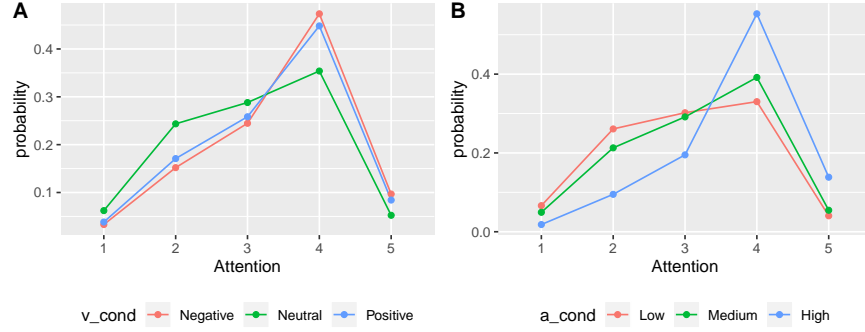


Figure 12: Attention scores (“The robot’s behavior draws my attention”) for different levels of valence (A) and arousal (B) conditioning. A) Pairwise comparisons revealed significantly higher scores for negative conditioning compared to neutral. B) Pairwise comparisons revealed significantly higher scores for high arousal conditioning compared to both medium and low.

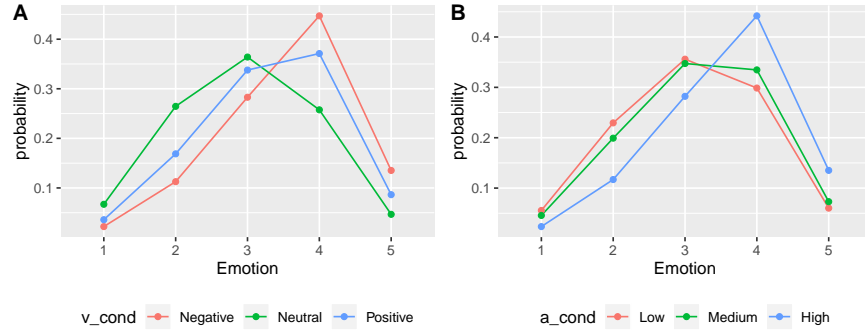


Figure 13: Emotion scores (“The robot’s expression is emotional”) for different levels of valence (A) and arousal (B) conditioning. A) Pairwise comparisons revealed significantly higher scores for negative and positive conditioning compared to neutral. B) Pairwise comparisons revealed significantly higher scores for high arousal conditioning compared to both medium and low.

Post hoc tests with Tukey’s p value adjustment for the arousal conditioning (a_cond) revealed statistically significant differences for the contrasts Low-High ($z = -5.33$, $p < 0.001$) and Medium-High ($z = -4.17$, $p < 0.001$). The result suggests that potentially animations sampled with larger radius from the latent space tend to draw participants’ attention more. The differences are presented in the model’s predictions in Fig. 12B and the results are summarized in Table 5.

The two ordered logistic regression models predicting the Emotion Likert scores (“The robot’s expression is emotional”) with the valence and arousal conditioning of the CVAE as a predictor respectively, detected statistically significant effects. The results are summarised in Table 4. Post hoc tests with Tukey’s p value adjustment on the levels of the the valence conditioning (v_cond) obtained statistically significant results for the contrasts Negative-Neutral ($z = 4.75$, $p < 0.001$) and Neutral-Positive ($z = -2.81$, $p = 0.01$). The results imply (Fig. 13A) that animations generated with negative or positive valence conditioning are perceived more as emotional compared to the ones generated with neutral valence conditioning. In the figure, a similar trend can perhaps be noted for Positive vs Negative, but this difference did not remain significant after the correction for multiple comparisons. The summary of the results is presented in Table 5.

For a_cond (arousal conditioning), statistically significant differences were detected for the contrasts Low-High ($z = -3.71$, $p < 0.001$) and Medium-High ($z = -2.85$, $p = 0.01$). This result suggests that animations sampled with a larger radius are perceived as more emotional. See also Fig. 13B, and Table5 for a summary of the results.

Regarding the proportional odds assumption, the likelihood ratio tests of the model terms produced p values greater than 0.05 for all four models, thus the null hypothesis cannot be rejected and the assumption is tenable.

6 Conclusion

In social robotics, human-robot interaction can be enhanced by endowing a robot with the ability to communicate using emotional body language (EBL). For robotic EBL to be engaging, it has to appear expressive, granular and interpretable in terms of the emotional class. To this aim, we implemented a Conditional Variational Autoencoder for the generation of multi-modal robotic EBL of targeted valence and arousal. The model was trained with a small set of robotic EBL animations designed for a Pepper robot by professional animators, including motion and eye LEDs colour sequences. The valence content of the generated animations was controlled by explicitly conditioning the training samples with scalar valence labels, while arousal conditioning was achieved by exploiting the geometry of the model’s latent space to guide the sampling process.

The interpretability of the generated animations was tested with a user evaluation study. The results provide support for valence conditioning which appears effective in differentiating positive or neutral from negative expressions. Similarly, arousal conditioning appears effective for differentiating high arousal from medium or low. However, only weak evidence were obtained for the differentiation between positive and neutral valence or between medium and low arousal. This limitation might be related to the composition of the training set, in which the representation of high valence and low arousal animations was lower than the rest of the classes [86]. Such imbalance could suggest a sample bias within the dataset, i.e., the model was not trained with enough examples from these two categories and did not learn to differentiate them well. This is an issue which can be resolved by collecting more labelled animations of high valence and low arousal. Nevertheless, this is consistent with previous studies using a NAO and a Robovie [110, 111] also report limitations in creating EBL expressions that are interpreted as of low arousal and high valence. Hence, it might be the case that this affect subspace is inherently difficult to represent, or perhaps emotional states from this affect subspace can be more successfully conveyed through other modalities, such as facial expression.

The analysis also showed that the generated animations do not appear to be less appealing compared to the designed animations in terms of Anthropomorphism and Animacy, either in the pretest phase or in the posttest phase. With regards to the impact of the robot’s behaviour on the user’s attention (presumably an aspect of believability), the results demonstrate that animations of more extreme levels of valence, or of high arousal, seem to draw more attention. Similarly, these animations are more strongly classified as emotional. A video with the physical robot executing several CVAE generated animations is available online⁷. The animations used for training, as well as the generated ones presented in the user study in this study can also be found online⁸.

Acknowledgments

This project received funding from the European Union’s Horizon 2020 research and innovation program under the Marie Skłodowska Curie grant agreement No 674868 (APRIL).

References

- [1] Cynthia Breazeal. Role of expressive behaviour for robots that learn from people. *Philosophical Transactions of the Royal Society B: Biological Sciences*, 364(1535):3527–3538, December 2009.
- [2] C. Bartneck and J. Forlizzi. A design-centred framework for social human-robot interaction. In *13th IEEE International Workshop on Robot and Human Interactive Communication*, pages 591–594, 2004.
- [3] Cynthia Breazeal, Kerstin Dautenhahn, and Takayuki Kanda. Social robotics. In Bruno Siciliano and Oussama Khatib, editors, *Springer Handbook of Robotics*, Springer Handbooks, pages 1935–1972. Springer International Publishing, Cham, 2016.
- [4] Terrence Fong, Illah Nourbakhsh, and Kerstin Dautenhahn. A survey of socially interactive robots. *Robotics and Autonomous Systems*, 42:143–166, 03 2003.
- [5] M. Karg, A. Samadani, R. Gorbet, K. Kühnlenz, J. Hoey, and D. Kulić. Body movements for affective expression: A survey of automatic recognition and generation. *IEEE Transactions on Affective Computing*, 4(4):341–359, 2013.
- [6] A. Kleinsmith and N. Bianchi-Berthouze. Affective body expression perception and recognition: A survey. *IEEE Transactions on Affective Computing*, 4(1):15–33, 2013.

⁷CVAE generated animation set video: <https://youtu.be/wmLT8FARSk0>

⁸REBL-Pepper Dataset: <https://github.com/minamar/rebl-pepper-data>

- [7] Zachary Witkower and Jessica L. Tracy. Bodily communication of emotion: Evidence for extrafacial behavioral expressions and available coding systems. *Emotion Review*, 11(2):184–193, 2019.
- [8] Mark Coulson. Attributing emotion to static body postures: Recognition accuracy, confusions, and viewpoint dependence. *Journal of Nonverbal Behavior*, 28(2):117–139, 2004-06-01.
- [9] Teodora Gliga and Ghislaine Dehaene-Lambertz. Structural encoding of body and face in human infants and adults. *Journal of Cognitive Neuroscience*, 17(8):1328–1340, 2005.
- [10] Julius Fast. *Body Language*. Henry Holt and Company, 1970.
- [11] Michael Argyle. *Bodily communication*. Methuen, London, UK, 1975.
- [12] Peter E. Bull. *Posture and gesture*. Pergamon Press, Oxford, UK, 1987.
- [13] Spiegel John and Machotka Pavel. *Messages of the body*. Free Press New York, 1974.
- [14] Nele Dael, Marcello Mortillaro, and Klaus R. Scherer. Emotion expression in body action and posture. *Emotion*, 12(5):1085–1101, October 2012.
- [15] Paul Ekman and Wallace V Friesen. Detecting deception from the body or face. *Journal of personality and Social Psychology*, 29(3):288, 1974.
- [16] Albert Mehrabian. *Nonverbal communication*. Aldine Transaction, New Brunswick, NJ, 2007.
- [17] Hillel Aviezer, Yaacov Trope, and Alexander Todorov. Body cues, not facial expressions, discriminate between intense positive and negative emotions. *Science*, 338(6111):1225–1229, 2012.
- [18] Beatrice de Gelder, Jan Van den Stock, Hanneke K.M. Meeren, Charlotte B.A. Sinke, Mariska E. Kret, and Marco Tamietto. Standing up for the body. Recent progress in uncovering the networks involved in the perception of bodies and bodily expressions. *Neuroscience & Biobehavioral Reviews*, 34(4):513 – 527, 2010.
- [19] R. Walk and K. L. Walters. Perception of the smile and other emotions of the body and face at different distances. *Bulletin of the Psychonomic Society*, 26(6):510–510, 1988.
- [20] Fritz Heider and Marianne Simmel. An experimental study of apparent behavior. *The American Journal of Psychology*, 57(2):243–259, 1944.
- [21] Luisa Damiano and Paul Dumouchel. Anthropomorphism in human–robot co-evolution. *Frontiers in Psychology*, 9:468, 2018.
- [22] Markus Koppensteiner. Perceiving personality in simple motion cues. *Journal of Research in Personality*, 45(4):358–363, 2011.
- [23] R. Hortensius, F. Hekele, and E. S. Cross. The perception of emotion in artificial agents. *IEEE Transactions on Cognitive and Developmental Systems*, 10(4):852–864, 2018.
- [24] E. Saad, J. Broekens, M. A. Neerinx, and K. V. Hindriks. Enthusiastic robots make better contact. In *2019 IEEE/RSJ International Conference on Intelligent Robots and Systems (IROS)*, pages 1094–1100, 2019.
- [25] C. L. Bethel and R. R. Murphy. Survey of non-facial/non-verbal affective expressions for appearance-constrained robots. *IEEE Transactions on Systems, Man, and Cybernetics, Part C (Applications and Reviews)*, 38(1):83–92, 2008.
- [26] K. Lee, W. Peng, S. Jin, and C. Yan. Can robots manifest personality? An empirical test of personality recognition, social responses, and social presence in human-robot interaction. *Journal of Communication*, 56:754–772, 2006.
- [27] L. Moshkina and R. C. Arkin. Human perspective on affective robotic behavior: a longitudinal study. In *2005 IEEE/RSJ International Conference on Intelligent Robots and Systems*, pages 1444–1451, 2005.
- [28] Rainer Reisenzein. A short history of psychological perspectives on emotion. In Rafael Calvo, Sidney D’Mello, Jonathan Gratch, and Arvid Kappas, editors, *The Oxford Handbook of Affective Computing*, chapter 2, pages 21–37. Oxford University Press, Inc., USA, 1st edition, 2015.
- [29] Paul Ekman and Daniel Cordaro. What is meant by calling emotions basic. *Emotion Review*, 3(4):364–370, 2011.
- [30] Jaak Panksepp and Douglas Watt. What is basic about basic emotions? Lasting lessons from affective neuroscience. *Emotion Review*, 3(4):387–396, 2011.
- [31] Paul Ekman. Universals and cultural differences in facial expressions of emotions. In *Nebraska Symposium on Motivation*, volume 19, pages 207–283, 1971.
- [32] James A Russell and Lisa Feldman Barrett. Core affect, prototypical emotional episodes, and other things called emotion: Dissecting the elephant. *Journal of Personality and Social Psychology*, 76 5:805–19, 1999.

- [33] James A Russell. Core affect and the psychological construction of emotion. *Psychological Review*, 110(1):145, 2003.
- [34] Albert Mehrabian and James A. Russell. *An approach to environmental psychology*. The MIT Press, 1974. Pages: xii, 266.
- [35] Trenton Schulz, Jim Torresen, and Jo Herstad. Animation techniques in human-robot interaction user studies: A systematic literature review. *ACM Transactions on Human-Robot Interaction*, 8(2):12:1–12:22, June 2019.
- [36] Andrea Kleinsmith, Issam Rebai, Nadia Berthouze, and Jean-Claude Martin. Postural expressions of emotion in a motion captured database and in a humanoid robot. In *Proceedings of the International Workshop on Affective-Aware Virtual Agents and Social Robots*, AFFINE '09, New York, NY, USA, 2009. Association for Computing Machinery.
- [37] Aryel Beck, Brett Stevens, Kim A. Bard, and Lola Cañamero. Emotional body language displayed by artificial agents. *ACM Transactions on Interactive Intelligent Systems*, 2(1):Article 2, March 2012.
- [38] Aryel Beck, Lola Cañamero, and K. A. Bard. Towards an affect space for robots to display emotional body language. In *19th International Symposium in Robot and Human Interactive Communication*, pages 464–469, 2010.
- [39] Daisuke Matsui, Takashi Minato, Karl F. MacDorman, and Hiroshi Ishiguro. Generating natural motion in an android by mapping human motion. In Hiroshi Ishiguro and Fabio Dalla Libera, editors, *Geminoid Studies: Science and Technologies for Humanlike Teleoperated Androids*, pages 57–73. Springer Singapore, Singapore, 2018.
- [40] Charles Darwin. *The expression of the emotions in man and animals*. John Murray, London, England, 1872.
- [41] Marco de Meijer. The contribution of general features of body movement to the attribution of emotions. *Journal of Nonverbal Behavior*, 13(4):247–268, December 1989.
- [42] H.G. Wallbott. Bodily expression of emotion. *European Journal of Social Psychology*, 28:879–896, 1998.
- [43] Kossinna Wasala, Rafael Gomez, Jared Donovan, and Marianella Chamorro-Koc. Emotion specific body movements: Studying humans to augment robots' bodily expressions. In *Proceedings of the 31st Australian Conference on Human-Computer-Interaction*, OZCHI'19, page 503–507, New York, NY, USA, 2019. Association for Computing Machinery.
- [44] Hatice Gunes and Massimo Piccardi. Bi-modal emotion recognition from expressive face and body gestures. *Journal of Network and Computer Applications*, 30:1334–1345, 11 2007.
- [45] Andrea Kleinsmith and Nadia Bianchi-Berthouze. Recognizing affective dimensions from body posture. In A. Paiva, R. Prada, and R. W. Picard, editors, *Affective Computing and Intelligent Interaction*, pages 48–58. Springer Berlin Heidelberg, 2007.
- [46] Markus Häring, Nikolaus Bee, and Elisabeth Andre. Creation and evaluation of emotion expression with body movement, sound and eye color for humanoid robots. In *IEEE International Workshop on Robot and Human Interactive Communication*, 07 2011.
- [47] S. Embgen, M. Luber, C. Becker-Asano, M. Ragni, V. Evers, and K. O. Arras. Robot-specific social cues in emotional body language. In *IEEE RO-MAN: The 21st IEEE International Symposium on Robot and Human Interactive Communication*, pages 1019–1025, September 2012.
- [48] Mustafa Suphi Erden. Emotional postures for the humanoid-robot Nao. *International Journal of Social Robotics*, 5(4):441–456, November 2013.
- [49] Christiana Tsiourti, Astrid Weiss, Katarzyna Wac, and Markus Vincze. Designing emotionally expressive robots: A comparative study on the perception of communication modalities. In *Proceedings of the 5th International Conference on Human Agent Interaction*, HAI '17, page 213–222, New York, NY, USA, 2017. Association for Computing Machinery.
- [50] Derek McColl and Goldie Nejat. Recognizing emotional body language displayed by a human-like social robot. *International Journal of Social Robotics*, 6(2):261–280, 2014.
- [51] M. Destephe, T. Maruyama, M. Zecca, K. Hashimoto, and A. Takanishi. Improving the human-robot interaction through emotive movements A special case: Walking. In *2013 8th ACM/IEEE International Conference on Human-Robot Interaction (HRI)*, pages 115–116, March 2013.
- [52] M. Destephe, A. Henning, M. Zecca, K. Hashimoto, and A. Takanishi. Perception of emotion and emotional intensity in humanoid robots gait. In *IEEE International Conference on Robotics and Biomimetics (ROBIO)*, pages 1276–1281, December 2013.

- [53] R. Laban. *Modern educational dance*. Macdonald & Evans Ltd, 1964.
- [54] H. Knight and R. Simmons. Expressive motion with x, y and theta: Laban Effort Features for mobile robots. In *The 23rd IEEE International Symposium on Robot and Human Interactive Communication*, pages 267–273, August 2014.
- [55] M. Sharma, D. Hildebrandt, G. Newman, J. E. Young, and R. Eskicioglu. Communicating affect via flight path: Exploring use of the Laban Effort System for designing affective locomotion paths. In *2013 8th ACM/IEEE International Conference on Human-Robot Interaction (HRI)*, pages 293–300, March 2013.
- [56] Julian M. Angel-Fernandez and Andrea Bonarini. Robots showing emotions. *Interaction Studies*, 17(3):408–437, January 2016.
- [57] Jekaterina Novikova and Leon Watts. A design model of emotional body expressions in non-humanoid robots. In *Proceedings of the Second International Conference on Human-agent Interaction, HAI '14*, pages 353–360, New York, NY, USA, 2014. ACM.
- [58] K. Takahashi, M. Hosokawa, and M. Hashimoto. Remarks on designing of emotional movement for simple communication robot. In *2010 IEEE International Conference on Industrial Technology*, pages 585–590, 2010.
- [59] Megumi Masuda, Shohei Kato, and Hidenori Itoh. Laban-based motion rendering for emotional expression of human form robots. In Byeong-Ho Kang and Debbie Richards, editors, *Knowledge Management and Acquisition for Smart Systems and Services*, pages 49–60, Berlin, Heidelberg, 2010. Springer Berlin Heidelberg.
- [60] Megumi Masuda, Shohei Kato, and Hidenori Itoh. A Laban-based approach to emotional motion rendering for human-robot interaction. In Hyun Seung Yang, Rainer Malaka, Junichi Hoshino, and Jung-Hyun Han, editors, *Entertainment Computing - ICEC 2010, 9th International Conference, ICEC 2010, Seoul, Korea, September 8-11, 2010. Proceedings*, volume 6243 of *Lecture Notes in Computer Science*, pages 372–380. Springer, 2010.
- [61] Megumi Masuda and Shohei Kato. Motion rendering system for emotion expression of human form robots based on laban movement analysis. In Carlo Alberto Avizzano and Emanuele Ruffaldi, editors, *19th IEEE International Conference on Robot and Human Interactive Communication, Viareggio, Italy, RO-MAN, 2010, September 13-15, 2010*, pages 324–329. IEEE, 2010.
- [62] Tatsuya Nomura and Akira Nakao. Comparison on identification of affective body motions by robots between elder people and university students: A case study in Japan. *International Journal of Social Robotics*, 2(2):147–157, 2010.
- [63] Toru Nakata, Taketoshi Mori, and Tomomasa Sato. Quantitative analysis of impression of robot bodily expression based on Laban movement theory. *Journal of the Robotics Society of Japan*, 19(2):252–259, 2001. In Japanese.
- [64] Angelica Lim and Hiroshi G. Okuno. A recipe for empathy. *International Journal of Social Robotics*, 7(1):35–49, November 2014.
- [65] Ádám Miklósi and Márta Gácsi. On the utilization of social animals as a model for social robotics. *Frontiers in psychology*, 3:75, 2012.
- [66] G. Lakatos, M. Gácsi, Veronika Konok, Ildikó Brúder, B. Bereczky, P. Korondi, and Á. Miklósi. Emotion attribution to a non-humanoid robot in different social situations. *PLoS ONE*, 9, 2014.
- [67] T. Shibata, T. Mitsui, K. Wada, A. Touda, T. Kumasaka, K. Tagami, and K. Tanie. Mental commit robot and its application to therapy of children. In *2001 IEEE/ASME International Conference on Advanced Intelligent Mechatronics.*, volume 2, pages 1053–1058 vol.2, 2001.
- [68] K. Wada, T. Shibata, T. Saito, and K. Tanie. Effects of robot-assisted activity for elderly people and nurses at a day service center. *Proceedings of the IEEE*, 92(11):1780–1788, 2004.
- [69] Toshiyo Tamura, Satomi Yonemitsu, Akiko Itoh, Daisuke Oikawa, Akiko Kawakami, Yuji Higashi, Toshiro Fujimooto, and Kazuki Nakajima. Is an entertainment robot useful in the care of elderly people with severe dementia? *The Journals of Gerontology Series A: Biological Sciences and Medical Sciences*, 59(1):M83–M85, 2004.
- [70] Alexander V Libin and Elena V Libin. Person-robot interactions from the robopsychologists’ point of view: The robotic psychology and robotherapy approach. *Proceedings of the IEEE*, 92(11):1789–1803, 2004.
- [71] Ollie Johnston Frank Thomas. *The illusion of life: Disney animation*. Disney Editions, 1995.
- [72] Jamy Li and Mark Chignell. Communication of emotion in social robots through simple head and arm movements. *International Journal of Social Robotics*, 3(2):125–142, April 2011.
- [73] Zane Thimmesch-Gill, Kathleen A. Harder, and Wilma Koutstaal. Perceiving emotions in robot body language: Acute stress heightens sensitivity to negativity while attenuating sensitivity to arousal. *Computers in Human Behavior*, 76:59 – 67, 2017.

- [74] Junchao Xu, Joost Broekens, Koen Hindriks, and Mark A. Neerinx. Mood contagion of robot body language in human robot interaction. *Autonomous Agents and Multi-Agent Systems*, 29(6):1216–1248, November 2015.
- [75] K. Itoh, H. Miwa, M. Matsumoto, M. Zecca, H. Takano, S. Roccella, M. C. Carrozza, P. Dario, and A. Takanishi. Various emotional expressions with emotion expression humanoid robot WE-4RII. In *IEEE Conference on Robotics and Automation, 2004. TExCRA Technical Exhibition Based.*, pages 35–36, 2004.
- [76] Jérôme Monceaux, Joffrey Becker, Céline Boudier, and Alexandre Mazel. Demonstration: First steps in emotional expression of the humanoid robot Nao. In *Proceedings of the 2009 International Conference on Multimodal Interfaces, ICMi-MLMI '09*, pages 235–236, New York, NY, USA, 2009. ACM.
- [77] T. Ribeiro and A. Paiva. The illusion of robotic life: principles and practices of animation for robots. In *2012 7th ACM/IEEE International Conference on Human-Robot Interaction (HRI)*, pages 383–390, March 2012.
- [78] S. Yohanan and K. E. MacLean. Design and assessment of the Haptic Creature’s affect display. In *2011 6th ACM/IEEE International Conference on Human-Robot Interaction (HRI)*, pages 473–480, 2011.
- [79] Michael Suguitan, Mason Bretan, and Guy Hoffman. Affective robot movement generation using CycleGANs. In *14th ACM/IEEE International Conference on Human-Robot Interaction, HRI 2019, Daegu, South Korea, March 11-14, 2019*, pages 534–535, 2019.
- [80] M. Marmpena, A. Lim, T. S. Dahl, and N. Hemion. Generating robotic emotional body language with variational autoencoders. In *2019 8th International Conference on Affective Computing and Intelligent Interaction (ACII)*, pages 545–551, 2019.
- [81] Michael Suguitan, Randy Gomez, and Guy Hoffman. Moveae: Modifying affective robot movements using classifying variational autoencoders. In *Proceedings of the 2020 ACM/IEEE International Conference on Human-Robot Interaction, HRI '20*, page 481–489, New York, NY, USA, 2020. Association for Computing Machinery.
- [82] Diederik P Kingma and Max Welling. Auto-encoding variational Bayes. *arXiv e-prints*, page arXiv:1312.6114, December 2013.
- [83] Danilo Jimenez Rezende, Shakir Mohamed, and Daan Wierstra. Stochastic Backpropagation and Approximate Inference in Deep Generative Models. *arXiv e-prints*, page arXiv:1401.4082, January 2014.
- [84] Diederik P. Kingma and Max Welling. An Introduction to Variational Autoencoders. *arXiv e-prints*, page arXiv:1906.02691, June 2019.
- [85] Kihyuk Sohn, Honglak Lee, and Xinchen Yan. Learning structured output representation using deep conditional generative models. In C. Cortes, N. D. Lawrence, D. D. Lee, M. Sugiyama, and R. Garnett, editors, *Advances in Neural Information Processing Systems 28*, pages 3483–3491. Curran Associates, Inc., 2015.
- [86] Mina Marmpena, Angelica Lim, and Torbjørn S. Dahl. How does the robot feel? Perception of valence and arousal in emotional body language. *Paladyn*, 9(1):168–182, 2018.
- [87] Geoffrey E. Hinton, Nitish Srivastava, Alex Krizhevsky, Ilya Sutskever, and Ruslan R. Salakhutdinov. Improving neural networks by preventing co-adaptation of feature detectors. *arXiv e-prints*, page arXiv:1207.0580, 2012.
- [88] Irina Higgins, Loic Matthey, Arka Pal, Christopher Burgess, Xavier Glorot, Matthew Botvinick, Shakir Mohamed, and Alexander Lerchner. β -vae: Learning basic visual concepts with a constrained variational framework. In *5th International Conference on Learning Representations*, 2017.
- [89] Christopher P. Burgess, Irina Higgins, Arka Pal, Loic Matthey, Nick Watters, Guillaume Desjardins, and Alexander Lerchner. Understanding disentangling in β -VAE. *arXiv e-prints*, page arXiv:1804.03599, April 2018.
- [90] Xavier Glorot and Yoshua Bengio. Understanding the difficulty of training deep feedforward neural networks. In *Proceedings of the Thirteenth International Conference on Artificial Intelligence and Statistics*, pages 249–256, 2010.
- [91] Diederik P. Kingma and Jimmy Ba. Adam: A method for stochastic optimization. *arXiv e-prints*, page arXiv:1412.6980, December 2014.
- [92] Christoph Bartneck, Elizabeth Croft, and Dana Kulic. Measurement instruments for the anthropomorphism, animacy, likeability, perceived intelligence, and perceived safety of robots. *International Journal of Social Robotics*, 1(1):71–81, 2009.
- [93] Alberto Betella and Paul F. M. J. Verschure. The affective slider: A digital self-assessment scale for the measurement of human emotions. *PLoS ONE*, 11(2):e0148037, Feb 2016.

- [94] Paulo Gomes, Ana Paiva, Carlos Martinho, and Arnav Jhala. Metrics for character believability in interactive narrative. In *Proceedings of the 6th International Conference on Interactive Storytelling - Volume 8230*, ICIDS 2013, page 223–228, Berlin, Heidelberg, 2013. Springer-Verlag.
- [95] Torrin M. Liddell and John K. Kruschke. Analyzing ordinal data with metric models: What could possibly go wrong? *Journal of Experimental Social Psychology*, 79:328 – 348, 2018.
- [96] Travis E Oliphant. *A guide to NumPy*, volume 1. Trelgol Publishing USA, 2006.
- [97] Pauli Virtanen, Ralf Gommers, Travis E. Oliphant, Matt Haberland, Tyler Reddy, David Cournapeau, Evgeni Burovski, Pearu Peterson, Warren Weckesser, Jonathan Bright, Stéfan J. van der Walt, Matthew Brett, Joshua Wilson, K. Jarrod Millman, Nikolay Mayorov, Andrew R. J. Nelson, Eric Jones, Robert Kern, Eric Larson, CJ Carey, İlhan Polat, Yu Feng, Eric W. Moore, Jake VanderPlas, Denis Laxalde, Josef Perktold, Robert Cimrman, Ian Henriksen, E. A. Quintero, Charles R Harris, Anne M. Archibald, Antônio H. Ribeiro, Fabian Pedregosa, Paul van Mulbregt, and SciPy 1.0 Contributors. Scipy 1.0: Fundamental algorithms for scientific computing in Python. *Nature Methods*, 17:261–272, 2020.
- [98] Wes McKinney et al. Data structures for statistical computing in Python. In *Proceedings of the 9th Python in Science Conference*, volume 445, pages 51–56. Austin, TX, 2010.
- [99] Fabian Pedregosa, Gaël Varoquaux, Alexandre Gramfort, Vincent Michel, Bertrand Thirion, Olivier Grisel, Mathieu Blondel, Peter Prettenhofer, Ron Weiss, Vincent Dubourg, et al. Scikit-learn: Machine learning in Python. *Journal of Machine Learning Research*, 12(Oct):2825–2830, 2011.
- [100] John D Hunter. Matplotlib: A 2D graphics environment. *Computing in Science & Engineering*, 9(3):90–95, 2007.
- [101] R Core Team. *R: A language and environment for statistical computing*. R Foundation for Statistical Computing, Vienna, Austria, 2019.
- [102] Hadley Wickham. *ggplot2: Elegant graphics for data analysis*. Springer-Verlag New York, 2016. <https://ggplot2.tidyverse.org>.
- [103] Alboukadel Kassambara. *rstatix: Pipe-friendly framework for basic statistical tests*, 2019. R package version 0.3.0. <https://CRAN.R-project.org/package=rstatix>.
- [104] W. N. Venables and B. D. Ripley. *Modern applied statistics with S*. Springer, New York, fourth edition, 2002.
- [105] R. H. B. Christensen. *ordinal: Regression models for ordinal data*, 2019. R package version 2019.12-10. <https://CRAN.R-project.org/package=ordinal>.
- [106] Russell Lenth. *emmeans: Estimated marginal means, aka Least-Squares Means*, 2019. R package version 1.4.3.01. <https://CRAN.R-project.org/package=emmeans>.
- [107] Hadley Wickham, Romain François, Lionel Henry, and Kirill Müller. *dplyr: A grammar of data manipulation*, 2019. R package version 0.8.3. <https://CRAN.R-project.org/package=dplyr>.
- [108] Jason Bryer and Kimberly Speerschneider. *likert: Analysis and visualization Likert items*, 2016. R package version 1.3.5. <https://CRAN.R-project.org/package=likert>.
- [109] Mina Marmpena, Fernando Garcia, and Angelica Lim. Generating robotic emotional body language of targeted valence and arousal with conditional variational autoencoders. In *Companion of the 2020 ACM/IEEE International Conference on Human-Robot Interaction, HRI '20*, page 357–359, New York, NY, USA, 2020. Association for Computing Machinery.
- [110] Aryel Beck, Antoine Hiolle, Alexandre Mazel, and Lola Cañamero. Interpretation of emotional body language displayed by robots. In *Proceedings of the 3rd International Workshop on Affective Interaction in Natural Environments*, pages 37–42. ACM, 2010.
- [111] K. Nakagawa, K. Shinozawa, H. Ishiguro, T. Akimoto, and N. Hagita. Motion modification method to control affective nuances for robots. In *2009 IEEE/RSJ International Conference on Intelligent Robots and Systems*, pages 5003–5008, 2009.